

Received: 27 October 2020

Revised: 26 February 2021



Accepted: 2 March 2021

DOI: 10.1111/gcb.15601



PRIMARY RESEARCH ARTICLE

How tree species, tree size, and topographical location influenced tree transpiration in northern boreal forests during the historic 2018 drought

Jose Gutierrez Lopez¹  | Pantana Tor-ngern^{2,3,4} | Ram Oren^{5,6}  | Nataliia Kozii¹ | Hjalmar Laudon¹ | Niles J. Hasselquist¹

¹Department of Forest Ecology and Management, Swedish University of Agricultural Sciences, Umeå, Sweden

²Department of Environmental Science, Chulalongkorn University, Bangkok, Thailand

³Environment, Health and Social Data Analytics Research Group, Chulalongkorn University, Bangkok, Thailand

⁴Water Science and Technology for Sustainable Environment Research Group, Chulalongkorn University, Bangkok, Thailand

⁵Division of Environmental Science & Policy, Nicholas School of the Environment, Duke University, Durham, NC, USA

⁶Department of Forest Science, University of Helsinki, Helsinki, Finland

Correspondence

Jose Gutierrez Lopez, Department of Forest Ecology and Management, Swedish University of Agricultural Sciences, Umeå, Sweden.

Email: gutloja@gmail.com, jose.lopez@slu.se

Funding information

Jane ja Aatos Erkon Säätiö; Swedish Research Council, Grant/Award Number: 2015-04791; Knut and Alice Wallenberg Foundation, Grant/Award Number: 2015.0047; Kempe Foundation; European Union's Horizon 2020, Grant/Award Number: 871126 and 871128; Swedish University of Agricultural Sciences; Formas; Future Forests; SKB; University of Helsinki

Abstract

Trees in northern latitude ecosystems are projected to experience increasing drought stress as a result of rising air temperatures and changes in precipitation patterns in northern latitude ecosystems. However, most drought-related studies on high-latitude boreal forests (>50°N) have been conducted in North America, with few studies quantifying the response in European and Eurasian boreal forests. Here, we tested how daily whole-tree transpiration (Q , Liters day⁻¹) and Q normalized for mean daytime vapor pressure deficit (Q_{DZ} , Liters day⁻¹ kPa⁻¹) were affected by the historic 2018 drought in Europe. More specifically, we examined how tree species, size, and topographic position affected drought response in high-latitude mature boreal forest trees. We monitored 30 *Pinus sylvestris* (pine) and 30 *Picea abies* (spruce) trees distributed across a topographic gradient in northern Sweden. In general, pine showed a greater Q_{DZ} control compared to spruce during periods of severe drought (standardized precipitation–evapotranspiration index: SPEI < -1.5), suggesting that the latter are more sensitive to drought. Overall, Q_{DZ} reductions (using non-drought Q_{DZ} as reference) were less pronounced in larger trees during severe drought, but there was a species-specific pattern: Q_{DZ} reductions were greater in pine trees at high elevations and greater in spruce trees at lower elevations. Despite lower Q_{DZ} during severe drought, drought spells were interspersed with small precipitation events and overcast conditions, and Q_{DZ} returned to pre-drought conditions relatively quickly. This study highlights unique species-specific responses to drought, which are additionally driven by a codependent interaction among tree size, relative topographic position, and unique regional climate conditions.

KEYWORDS

drought, Norway spruce, sap flow, Scots pine, topographic position, tree size, tree transpiration

This is an open access article under the terms of the Creative Commons Attribution-NonCommercial-NoDerivs License, which permits use and distribution in any medium, provided the original work is properly cited, the use is non-commercial and no modifications or adaptations are made.

© 2021 The Authors. *Global Change Biology* published by John Wiley & Sons Ltd.

1 | INTRODUCTION

The historical 2018 drought registered across Central and Northern Europe, and considered the most severe in the last 250 years (MSB, 2017; Schuldt et al., 2020), had major impacts on northern boreal forests, including severe tree-level stress, record low stream flows, and changes in water and carbon fluxes (Gómez-Gener et al., 2020; Hari et al., 2020; Lindroth et al., 2020; Schuldt et al., 2020). Globally, boreal forests cover approximately 12% of the earth's surface (Launiainen et al., 2019), representing the second largest biome behind tropical forests (Bonan, 2008). They are located between 45° and 70° north latitude, with two-thirds of all boreal forests located in Eurasia (Larsen, 1980). Given their wide distribution, boreal forests regulate water and energy fluxes over a vast area and thus play an important role in global hydrology and climatology (Baldocchi et al., 2000; Bonan, 2008; Chalita & Le Treut, 1994; Chen et al., 2018; Price et al., 2013). Boreal forests also play a critical role in the global carbon cycle (Goodale et al., 2002); sequestering ca. 0.5 petagrams of carbon per year, and storing approximately one-third of the global terrestrial carbon (Bradshaw & Warkentin, 2015; Bradshaw et al., 2009; Pan et al., 2011).

Boreal forests are experiencing rapid climate change including rising temperatures (Choi & Kim, 2018; Price et al., 2013), altered precipitation patterns (Kjellström, 2004), and an increased frequency of summer drought stress (Ma et al., 2012). High latitude ecosystems are projected to experience the greatest rise in temperatures (IPCC, 2013), and correspondingly this could result in an increase in the evaporative demand leading to enhanced drought stress for plants (Angert et al., 2005; Dai, 2013; Williams et al., 2013). Additionally, several studies indicate that water availability from precipitation may also become limiting for tree growth in boreal forests in a future climate (Christidis et al., 2015; D'Orangeville et al., 2018; Dai, 2013; Huang & Xia, 2019; Price et al., 2013; Walker et al., 2015; Way et al., 2013). Although the total amount of summer precipitation is not projected to change significantly in the future, the timing and magnitude of summer precipitation are expected to be altered with longer periods without precipitation interspersed with large, infrequent rain events (IPCC, 2013; Kjellström, 2004). Such changes to the hydrological cycle may have profound consequences on tree transpiration and forest growth.

From a phyto-centric perspective, drought can be described as an extended period of stress resulting from enhanced atmospheric demand (i.e., atmospheric drought) and low soil moisture (for further readings, see: McDowell et al., 2008; Rowland et al., 2015). In North American boreal forests, increasing frequency of drought stress has led to tree mortality (Peng et al., 2011) as well as an overall reduction in carbon storage and forest productivity (Barber et al., 2000; Hogg et al., 2008; Ma et al., 2012; Silva et al., 2010). Additionally, droughts can have severe negative socioeconomical and ecological consequences at local, regional, and global scales (Hogg et al., 2002; Van Loon et al., 2016; Vörösmarty et al., 2010). In contrast to the relatively well-studied conditions in North America (e.g., Peng et al., 2011; Price et al., 2013; Way et al., 2013), less is known about how

trees in Fennoscandian boreal forests will respond to drought. For example, in central Sweden, reductions in soil moisture and high vapor pressure deficit (VPD, kPa) have shown to reduce transpiration in mature Norway spruce (*Picea abies*, hereafter spruce) and Scots pine (*Pinus sylvestris*, hereafter pine) trees (Čermák et al., 1995; Cienciala et al., 1997, 1999; Lagergren & Lindroth, 2002), and similar trends have been observed in other conifers in Siberian (Kropp et al., 2017) and Russian boreal forests (Oltchev et al., 2002). However, no studies have addressed the relationships between tree size, species, and the effect of these factors on trees response to drought (but see: Lagergren & Lindroth, 2004). Additionally, because of ecological and environmental differences driven by the air stream over the Atlantic, specifically warmer temperatures and higher precipitation (Boonstra et al., 2016), it is likely that forests in Fennoscandia and other Eurasian boreal forests may respond differently to drought than those in North America, yet we have little empirical data for testing mechanistic models projecting the response of Fennoscandian boreal forests to a warmer and drier future.

Spruce trees tend to grow and thrive in more fertile, mesic environments, and are thus dominant at lower topographic positions compared to pine trees, which can grow in more nutrient-poor, xeric environments that are often in upland areas within a watershed (Cienciala et al., 1999; Gartner et al., 2009; Lagergren & Lindroth, 2002). It has also been shown that drought stress tends to increase with elevation (Hawthorne & Miniati, 2018), which results from gravitational forces moving water toward the lower parts of the watershed (Fetter, 2001; Hillel, 2004). Yet, how different species will respond to drought based on their topographic location, has not been fully studied. Thus, species characteristics and site-specific factors including topography indicate that pine should be more resilient to drought stress compared to spruce. Previous studies have also shown that trees of different size respond differently to drought, with larger trees being more vulnerable to drought as a result of greater exposure to atmospheric evaporative demand (Bennett et al., 2015; Pretzsch et al., 2018; Stovall et al., 2019). However, how all these factors, tree species, tree size, and topographic position, influence drought responses remain largely unknown, particularly within the Fennoscandian context. The effects of tree size in particular have not been well studied, in part due to the even-aged diameter distribution commonly observed in Swedish managed forests (Cienciala et al., 1997, 1999; Kozii et al., 2020; Laudon et al., 2013).

In this study, we take advantage of 3 years of continuous measurements from a large network of sap flow sensors in a boreal forest in northern Sweden to address the following questions: (1) did the severe drought in 2018 result in enhanced drought stress as indicated by reduced whole-tree transpiration?, (2) was there a species-specific and tree size-specific response to severe drought?, and (3) did topographic position within the watershed played a role in drought response? Measurements of whole-tree transpiration were made between 2017 and 2019, which represents a cold, wet summer (2017), a historical severe summer drought (2018), and a warm year (2019). We hypothesized (H1) that mean annual whole-tree

transpiration would be reduced during the 2018 drought as a result of abnormally high temperatures and enhanced atmospheric drought and low soil moisture. Additionally, we expected pine to be more resilient to drought stress compared to spruce due to their documented higher tolerance to low soil moisture (Sutinen & Middleton, 2020) and lower water use requirements due to a lower leaf area, compared to spruce. We further hypothesized that (H2) larger trees of both species will be more sensitive to drought stress because of larger water needs and overall greater exposure to evaporative demand than smaller trees. Finally, we hypothesized that (H3) trees in higher elevations (i.e., upland locations) will show greater reductions in transpiration, compared to trees in lower topographic positions, because of lower soil moisture in upland locations during extreme drought conditions.

2 | MATERIALS AND METHODS

2.1 | Study site

This study was conducted in the 14 ha C2 subcatchment, within the larger 67 km² Krycklan Catchment study area (Kozii et al., 2020; Laudon et al., 2013) in northern Sweden (64.256°N, 19.775°E, Figure 1). The Krycklan catchment is one of the most well-instrumented catchments in northern latitudes with continuous climatic and hydrological measurements dating back to the early 1980s (Laudon et al., 2013). Mean annual temperature is 2.1°C and mean annual precipitation is 619 mm year⁻¹ based on 33 years of measurements (1985–2019). Approximately 40% of the annual precipitation falls in the form of

snow, with snow accumulation beginning in early November and lasting until the end of April.

Soils within the C2 subcatchment are dominated by glacier till (84%), with an organic layer that is on average 8 cm thick (Ivarsson & Johnsson, 1988). The subcatchment is characterized by a near continuous cover of old (>120 year) mixed forest of *Picea abies* (61%), *Pinus sylvestris* (34%), and *Betula* spp. (5%; Laudon et al., 2013). The understory consists of a rich layer of bilberry (*Vaccinium myrtillus*) and lingonberry (*Vaccinium vitis-idaea*) with mosses (*Pleurozium schreberi* and *Hylocomium splendens*) in the bottom layer. In 2014, the integrated carbon observation system (ICOS) ecosystem-atmosphere station was established within the subcatchment which provides continuous data on greenhouse gases, water, and energy fluxes as well as meteorological, vegetation, and soil environmental variables (ICOS, 2019).

2.2 | Measurements of stand characteristics and sapwood area

Measurement of site characteristics, which include stand density, basal area, and sapwood area (A_s , m²), was made from seven, 10 m radius permanent plots distributed across the subcatchment (Figure 1). These permanent plots are part of a larger scale, long-term forest monitoring program across the entire Krycklan watershed, which consists of a total of 556 permanent plots arranged in a square grid with 350 m spacing between adjacent plots. In the fall of 2014 and spring of 2015, DBH, height, and species identity were recorded for each tree within each of the 556 permanent plots. In

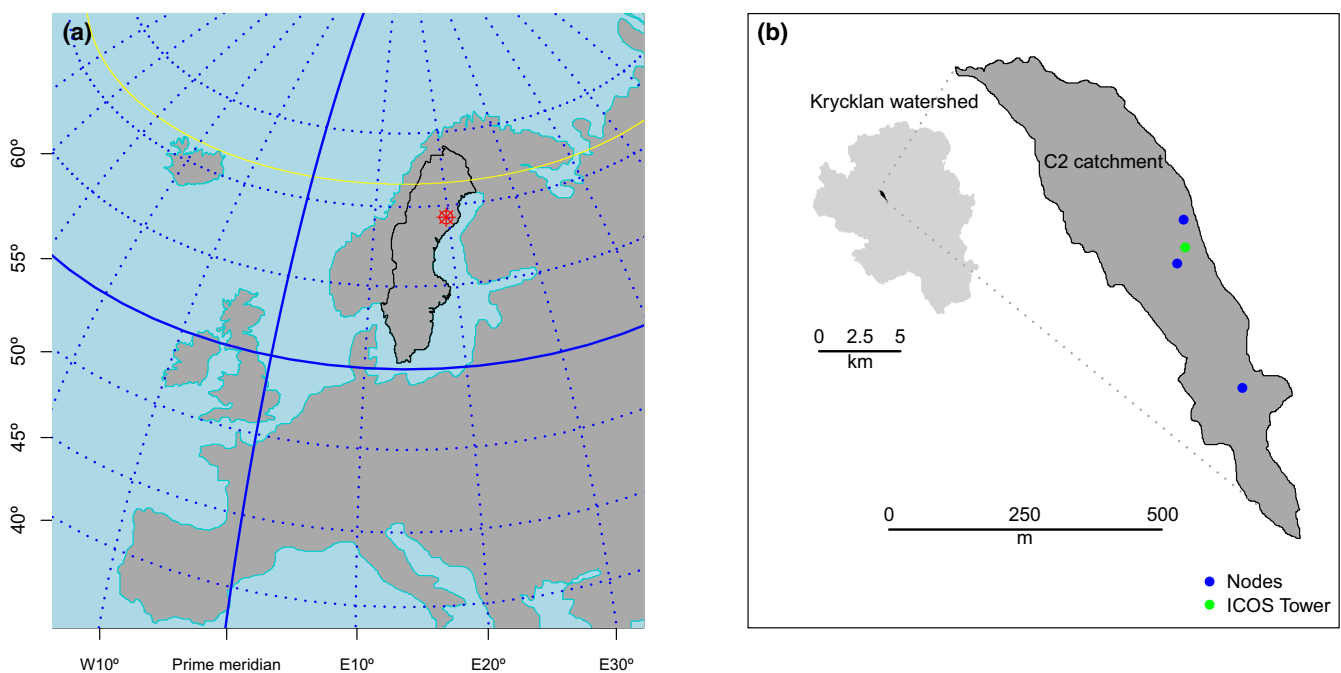


FIGURE 1 (a) Geographical location of the study site (red star). Yellow line indicates the polar circle. (b) Location of C2 subcatchment inside the Krycklan Experimental Watershed. Blue dots show the relative position of each the monitoring nodes the green circle the ICOS tower

2017, tree cores were collected from individual trees to determine the sapwood depth (D_s , cm) of both pine and spruce ($n = 30$ per species). For each tree core, D_s was estimated visually and recorded on site using a light-diffusion method (Long & Dean, 1986; Wengert, 1976). D_s was then converted to sapwood area (A_s , m²). Equation and parameters are shown in Appendix S1.

2.3 | Environmental data

Environmental data used in this study include photosynthetic active radiation (PAR, $\mu\text{mol m}^{-2} \text{s}^{-1}$; Apogee SQ110), air temperature (AirT, °C; Rotronic MP201H), relative humidity (RH, %; Rotronic MP201H), net radiation (NetRad, $\text{W m}^{-2} \text{s}^{-1}$; CNR4 Kipp & Zonen), vapor pressure deficit (VPD, kPa), soil heat flux (G, $\text{Joules m}^{-2} \text{s}^{-1}$; Hukseflux HFP01SC), and volumetric water content at four soil depths (5, 15, 25, and 50 cm; DeltaT Devices ML2). All environmental data were obtained from the ICOS portal, Svartberget station (ICOS, 2019). Volumetric water content was converted to soil saturation (S , unitless), according to van Genuchten (1980). Soil saturation was estimated for the four soil depths in which volumetric water content was measured, but in this study, we primary focused on S within the upper 15 cm of the soil profile.

Due to differences in day-length conditions during the growing season, we estimated mean day-length-normalized PAR (PAR_Z , $\mu\text{mol m}^{-2} \text{s}^{-1}$) and VPD (D_Z , kPa). First, daytime was defined as the time when PAR was higher than $20 \mu\text{mol m}^{-2} \text{s}^{-1}$ (which was sufficient to eliminate false positives, i.e., overcast conditions with low light). Once the length of a day was defined, we estimated mean PAR_Z or D_Z , by multiplying their mean by the ratio of the day length (i.e., the proportion of 24 h that were labeled as day).

2.4 | Sap flux measurements

Whole-tree transpiration (Q , L day^{-1}) was estimated using a network of continuous sap flux measurements. Within the C2 subcatchment, we selected three locations (hereafter: nodes) to measure tree-level transpiration. Each node was located along a topographic gradient: shoulderslope (high), backslope (middle), and footslope (low) (285–260 m a.s.l., respectively). Within each node (25 m radius), we selected 20 trees (10 pine and 10 spruce) that represented the diameter distribution of trees in the entire C2 subcatchment. Sap flux density (J_s , $\text{cm}^3 \text{cm}^{-2} \text{h}^{-1}$) was measured at breast height (1.3 m above the ground) using custom-made heat dissipation-type sap flow sensors (Granier, 1985, 1987; Gutiérrez López, 2015). These sensors were installed on selected trees and all sensors were covered with reflective insulation to minimize the effect of natural temperature gradients. To account for radial and circumferential variability in J_s (Berdanier et al., 2016; Caylor & Dragoni, 2009; Granier et al., 1994; Wullschlegel & King, 2000), we installed sensors at four sapwood depths (i.e., 0–20 mm, 20–40 mm, 40–60 mm, and 60–80 mm) in a subset of trees (five per species per node). Additionally, we installed

sensors in the four cardinal directions on the stems of six selected trees ($n = 3$ per species). In total, we installed 150 sap flow sensors on 60 trees (20 trees per node). Differential voltage (DiffV, mV) between the heated and the reference probe was read every 30 s and stored as 30-minute averages using a data logger (CR1000X, Campbell Scientific) per node.

2.5 | Wounding drift correction for sap flux measurements

To correct for wounding drift, that is, the cumulative changes in sensor sensibility over time due to the formation of scar tissue or tyloses (Flo et al., 2019; Kitin et al., 2010; McElrone et al., 2010; Peters et al., 2018), we deployed eight additional HD sensors in the Spring of 2019 on eight trees ($n = 4$ per species) that already had HD sensors from the beginning of this study. New HD sensors were installed in the outer 0–20 mm of sapwood and data were collected during the entire 2019 growing season (May–October). Comparison of old versus new J_s and equations used to correct for wounding drift are shown in Appendix S2.

2.6 | Data processing

All data were processed with scripts developed for R 3.6.3 (R Core Team). Using environmental data obtained from the ICOS-Sweden, Svartberget station, we calculated potential evapotranspiration at 30 min of intervals (ET_0 , mm day^{-1}) following the Penman–Monteith equation:

$$\text{ET}_0 = \frac{0.408\Delta (R_n - G) + \gamma \frac{900}{T_{\text{Air}} + 273} u_2 (e_s - e_a)}{\Delta + \gamma (1 + 0.34u_2)}, \quad (1)$$

where Δ is the slope of the vapor pressure curve ($\text{kPa } ^\circ\text{C}^{-1}$), R_n the net radiation ($\text{MJ m}^{-2} \text{day}^{-1}$), G the soil heat flux density ($\text{MJ m}^{-2} \text{day}^{-1}$), γ the psychrometric constant ($0.065 \text{ kPa } ^\circ\text{C}^{-1}$) estimated at an elevation of 275 m a.s.l. Air temperature (T_{Air} , °C), wind speed (u_2 , m s^{-1}), saturation vapor pressure (e_s , kPa), and the actual vapor pressure (e_a , kPa).

After an initial filter to remove outliers and to clean up data, raw data (DiffV, mV) from HD sensors were converted to J_s using the empirical equation (Granier, 1985), adjusted to our desired units (i.e., $\text{cm}^3 \text{cm}^{-2} \text{h}^{-1}$) as:

$$J_s = 42.8 \times \left(\frac{\text{DiffV}_m - \text{DiffV}}{\text{DiffV}} \right)^{1.231}, \quad (2)$$

where DiffV_m is the maximum voltage difference under zero flow conditions which occur at night and when ET_0 is low. DiffV_m was determined by first selecting raw DiffV data that occurred when ET_0 was zero for at least two consecutive hours. We then fitted a LOESS line (Cleveland, 1979, 1981; R parameters: Gaussian, surface = direct, statistics = exact, span = 0.02) through the selected DiffV data, which

allowed us to estimate a continuous and robust maximum DiffV_m during contrasting environmental conditions that are typical of northern latitude ecosystems (i.e., extreme temperature changes and variation of daylight hours).

Radial J_s profiles' functions were fit to each measurement (at 30 min of intervals) following the protocols defined for conifers (Caylor & Dragoni, 2009). Sapwood area (A_s , in cm²) was estimated for each of the 60 monitored trees using the respective allometric equations for each species (Appendix S1). Q (L day⁻¹) for each tree was estimated as follows: first, we split each sapwood depth (D_s , cm) into 50 equal subsections, then we integrated the product of J_s (predicted with radial profile equations) and A_s of each D_s subsection. Q was estimated for each 30 min of interval, and then summed up per day. Finally, daily Q for each tree was normalized for D_z (Q_{Dz} , L day⁻¹ kPa⁻¹) by dividing daily Q by D_z (mean day-length-normalized VPD, kPa). Q_{Dz} minimizes phenological and seasonal effects of Q and thus was used to assess species-specific drought responses of pine and spruce during the 2018 drought. Q_{Dz} is also an approximation to canopy conductance (without accounting for the conductance coefficient as a function of temperature; Phillips & Oren, 1998), and it is similar to uses in several previous studies (Damour et al., 2010; Dang et al., 1997; Ewers & Oren, 2000; Kropp et al., 2017; Lagergren & Lindroth, 2002).

2.7 | Long-term environmental records and drought index

Long-term (1985–2019) precipitation (pp, mm day⁻¹), RH, AirT, and calculated VPD (Zotarelli et al., 2009) were obtained from the Svartberget Research Station, located 1.2 km from our study site. To estimate long-term ET₀, we fitted an exponential model between VPD and ET₀ for the 2016–2019 time period (see Appendix S3 for details) and used this model to predict long-term ET₀ between 1985 and 2015. Using ET₀ and precipitation data from the 33 years period (1985–2019), we calculated a standardized precipitation–evaporation index on a weekly timescale (SPEI, Vicente-Serrano et al., 2010). Environmental data during the 2018 drought are compared to the long-term averages in Appendix S3. To assess the effects of drought, weekly SPEI estimates in 2018 were split into the four standard ranges: severe drought (SPEI ≤ -1.5), mild drought (-1.5 > SPEI < -0.5), normal (-0.5 ≥ SPEI < 0.5), and wet (SPEI ≥ 0.5).

2.8 | Statistical analyses

Prior to statistical analyses, all datasets were tested for normal distribution using Shapiro–Wilk test. Data used in most statistical analyses corresponded to the snow-free period (April–October). Additionally, for statistical analyses, we omitted data from overcast days which were days that met any of the following criteria: PAR_Z < 30 μmol m⁻² s⁻¹, D_z < 0.1 kPa, pp > 1 mm. To assess the

effects of species, tree size, and topographic position, we fitted a mixed model using JMP PRO 15 (SAS Institute Inc.), where D_z , PAR_Z, S, SPEI range, tree size, and topographic position were the independent variables. To account for natural variability over time, and among trees, individual trees and week of the year were considered random variables. Additionally, we tested the effects of all relevant interactions, including species + SPEI range + tree size and species + SPEI range + topographic position. The model was fitted for all monitored years (2017, 2018, and 2019) to highlight year-specific effects, and merging all years to further increase the predicting power of the model and interactions of interest. Further details and mixed model outputs are shown in Appendix S4.

3 | RESULTS

3.1 | Environmental conditions

In 2018, annual average ET₀ was 7% higher than the 33 years of long-term mean (1.55 and 1.44 ± 2.5 mm day⁻¹; respectively). Moreover, during the severe drought in 2018, there were two periods (May 15–June 17, and June 28–July 22) in which the SPEI drought index was the lowest during the 33 years of record (Figure 2a). In general, soil saturation (S) was highest during spring after snow melt. As a result of rapid warming in early spring, S was greater in 2018 compared to 2017 and 2019 (Figure 2b). In 2018, mean annual temperature was ca. 30% higher than the 33 years of period (3.2 and 2.28 ± 0.95°C; respectively) with the highest mean daily temperature (24.7°C) during the last 33 years being recorded on July 17, 2018 (Appendix S3). Annual precipitation in 2018 was 16% lower than the long-term average (543 mm year⁻¹) and was the fourth driest year since 1984 (Figure 2c). During April–October, total precipitation was 18% lower in 2018 compared to the long-term average (328 and 371 mm year⁻¹, respectively). There were no differences in PAR_Z among years, and in general, annual mean PAR_Z was 350 μmol m⁻² s⁻¹ (Figure 2d). Annual D_z was on average 35% higher in 2018 compared to 2017 and 2019 ($p < 0.001$; Figure 2d).

3.2 | Whole-tree transpiration

In general, mean whole-tree transpiration (Q , L day⁻¹) including all monitored trees and across years was lower in 2017 (4.9 L day⁻¹) compared to 2018 and 2019 (5.44 and 5.8 L day⁻¹, respectively), although their difference was only marginally significant ($p = 0.05$, Figure 3). Mean whole-tree transpiration was reduced during the first severe drought period in 2018 (May 15–June 17), yet quickly recovered in response to c. 40 mm of cumulative precipitation at the end of the drought period. After normalizing Q for variations in D_z (Q_{Dz}), mean daily Q_{Dz} during the snow-free period was significantly lower ($p < 0.0001$) in 2018 (13 L day⁻¹) compared to 2017 (17.8 L day⁻¹) and 2019 (14.9 L day⁻¹).

FIGURE 2 Summary of environmental variables within C2 subcatchment during the study period; (a) weekly SPEI drought index, (b) average soil saturation (S , unitless) in the top 15 cm of the soil profile, (c) weekly precipitation with precipitation $<10 \text{ mm week}^{-1}$ in red and precipitation $>10 \text{ mm week}^{-1}$ in blue, and (d) day-length-normalized mean VPD (D_z) and PAR (PAR_z)

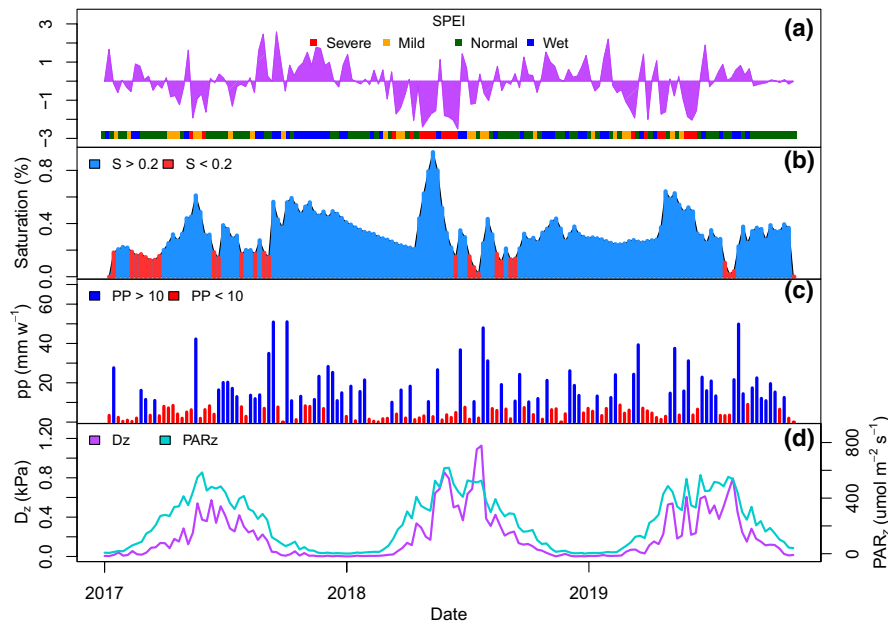
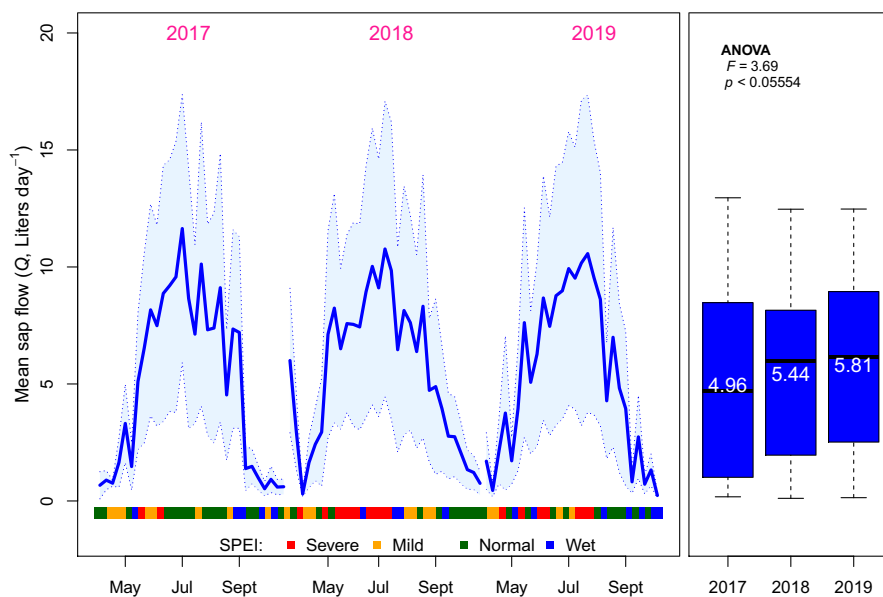


FIGURE 3 Weekly average of daily whole-tree transpiration (Q , L day^{-1}) during the snow-free period (April–October). The area inside dotted lines is the mean average deviation for all the values within that week. Boxplots on the right side show the average for each year (April–October). Overcast days (i.e., precipitation greater than 1 mm day^{-1} and $D_z < 0.1 \text{ kPa}$) were omitted from the analysis



3.3 | Tree size and species response

In 2018, Q_{DZ} in both tree species (including all tree sizes) was reduced by c. 30% during severe drought conditions (33% and 29%, for pine and spruce, respectively, $p < 0.0001$ for both species) relative to normal drought conditions (i.e., SPEI: -0.5 to 0.5 ; Figure 4). According to our mixed model, Q_{DZ} was significantly different (and lower during severe drought) across drought ranges in 2018 and 2019, and by-species analysis showed that spruce was consistently and significantly lower across years (Appendix S4). The combined analysis of drought range and tree size (DR + Tree size interaction, Appendix S4) showed that in 2018 tree size played a key role in drought response with both large and small trees of both species showing a greater response to drought. Further split by species,

the analysis showed that while not significantly different for pine nor spruce ($p = 0.59$; Appendix S4), the reduction in Q_{DZ} of pine during severe drought was more pronounced in large compared to medium and small trees. Conversely, the opposite was observed for spruce and a greater reduction in Q_{DZ} was observed in small spruce trees compared to medium and large trees as shown in Figure 4.

3.4 | Effects of topographic position on tree response

There was a general difference in mean Q_{DZ} (including both species) by topographic position that was reflected in the significant

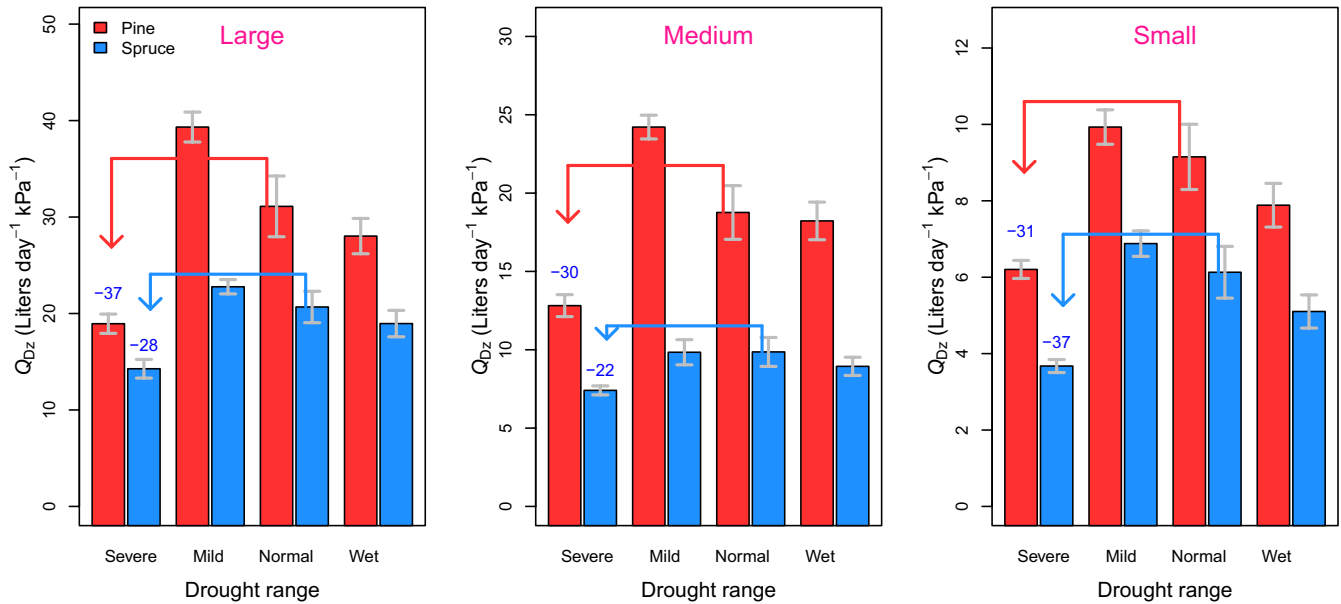


FIGURE 4 Response of VPD-normalized sap flow (Q_{DZ} , Liters day⁻¹ kPa⁻¹) to different drought severity conditions in 2018 (severe drought: SPEI < -1.5, mild drought: SPEI \geq -1.5 and < -0.5, normal: SPEI \geq -0.5 and < 0.5, wet: SPEI \geq 0.5) among different size trees (large > 25 DBH; medium = 15 < x < 25 DBH, and small < 15 DBH). Numbers on top of the severe drought bars indicate the respective percent difference with respect to Q_{DZ} under normal SPEI

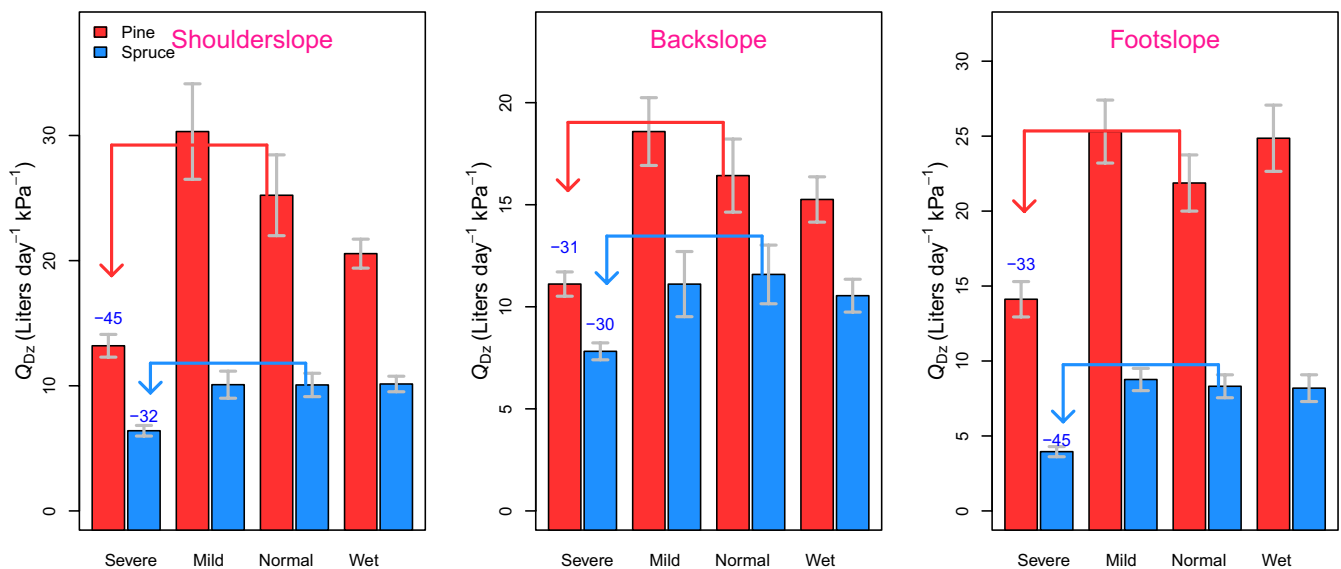


FIGURE 5 Response of VPD-normalized sap flow (Q_{DZ} , Liters day⁻¹ kPa⁻¹) to different drought severity conditions in 2018 (severe drought: SPEI < -1.5, mild drought: SPEI \geq -1.5 and < -0.5, normal: SPEI \geq -0.5 and < 0.5, wet: SPEI \geq 0.5) among different topographical locations within the C2 subcatchment (backslope = 285, shoulderslope = 270, and footslope = 260 m a.s.l., approx.). Numbers on top of the severe drought bars indicate the respective percent difference with respect to Q_{DZ} under normal SPEI

difference observed by our analysis ($p < 0.0001$, all years, Appendix S4). Overall, mean Q_{DZ} was greater at shoulderslope (high elevation) and lower at backslope (medium elevation). However, the combined analysis of drought range and topographic position showed that Q_{DZ} was generally lower at all topographic positions during severe drought in 2018 ($p = 0.002$; Appendix S4), as shown in Figure 5.

Further analysis by species showed that pine had the largest reduction in Q_{DZ} in shoulderslope (-45%) compared to backslope and footslope (31% and 33%; respectively). In contrast, Q_{DZ} in spruce trees was reduced by 45% in footslope, whereas the reductions in Q_{DZ} in the shoulderslope and backslope were not as great during severe drought conditions (32% and 30%, respectively; Figure 5).

4 | DISCUSSION

Although mean annual whole-tree transpiration (Q , $L \text{ day}^{-1}$) was lower in 2018 compared to 2019, this reduction was only marginally significant. Interestingly, mean annual Q was greater in 2018 compared to 2017, but the lower mean annual Q of 2017 was the result of a higher number of overcast days. Taken together, these findings led us to reject our first hypothesis that the severe drought in 2018 would result in enhanced drought stress as indicated by reduced transpiration. Although this finding is in contrast to previous studies that have reported reduced transpiration in response to drought in North America (Hogg et al., 2002, 2008), northern Europe (Gartner et al., 2009), and southern Sweden (Cienciala et al., 1997, 1999; Hasper et al., 2016; Lagergren & Lindroth, 2002), it is consistent with results showing nearly invariable transpiration in both temperate and boreal stands (Oishi et al., 2010; Torngern et al., 2017; Ward et al., 2018). One possible explanation for why transpiration remains relatively invariable over large range of annual or growing seasons may be due to the common occurrence of overcast conditions and small frequent rain events that in turn can influence VPD and atmospheric water demand, which ultimately regulate stomatal conductance as VPD increases. As consequence, normalizing whole-tree transpiration by daily variations in D_z (Q_{DZ} , $L \text{ day}^{-1} \text{ kPa}^{-1}$), we found that the 2018 drought resulted in a significant reduction in Q_{DZ} in 2018 compared to 2017 and 2019, consistent with reductions in conductance observed in central Sweden (Cienciala et al., 1997, 1999; Lagergren & Lindroth, 2002).

In addition to atmospheric conditions, the period of time without precipitation is also likely to affect how trees respond to drought. In 2018, there were two severe drought periods ($\text{SPEI} \leq -1.5$), with the first one from May 15 to June 17 and the second period between June 28 and July 22 (Figure 2a). During both drought periods, there were minor precipitation events ($\text{max } 2.5 \text{ mm day}^{-1}$), whereas the end of each drought period was characterized by large rain events which recharged the soil water content (Figure 2b). Several studies point to a growing risk of tree mortality in northern latitude ecosystems as a result of increasing temperatures and extended periods without precipitation (Hogg et al., 2002; Montwé et al., 2016; Williams et al., 2013; Peng et al., 2011; Price et al., 2013; Soja et al., 2007; Way et al., 2013). However, using a long-term dataset (1983–2019), we found that continuous clear sky conditions with no precipitation are extremely rare at our study site, with <1% of the periods analyzed comprised of 10 successive days, or longer, of clear sky (Appendix S3). While there is no general consensus on how long drought conditions have to persist in order to cause hydraulic failure and plant death, trees regulate water use such that hydraulic failure is avoided while maintaining some photosynthesis. Such regulation is strongly driven by species-specific factors such as trees behavior along the iso/anisohydric continuum (for topic review see: Martínez & García, 2017; McDowell et al., 2008), or size- and age-related changes in leaf morphology and function (Niinemets, 2002). Regardless of the behaviors, the increase in transpiration following drought-breaking precipitation may trigger a delayed response on available soil moisture and atmospheric conditions, resulting in a

carryover effect after a drought period (Ewers et al., 1999). Such carryover effect may include the time required for a recovery of xylem function and improved root–soil contact. Indeed, when a drought spell in central Sweden was interrupted by precipitation, reductions in mature pine and spruce transpiration was observed (Cienciala et al., 1997). However, in this study, we show that small, infrequent rain events during the most severe drought conditions in 2018 were sufficient to maintain tree transpiration, highlighting the ability of small precipitation and overcast days to reset drought spells.

Higher water demands due to higher leaf area or tree size can influence the way species respond to drought. In Scandinavian boreal forests, spruce tends to have a higher leaf area compared to pine of a given size, and commonly grows in stands reaching higher leaf area index (LAI; Cienciala et al., 1997; Goude et al., 2019). Spruce, however, has lower stomatal conductance, as indicated by its lower Q_{DZ} (Figures 4 and 5). Furthermore, as previously mentioned, age- or size-related leaf morphology and function, such as reductions in conductance (Lai et al., 2000; Schäfer et al., 2000), can compensate for hydraulic risk potentially associated with higher LAI or conductance. The way in which trees are able to access available soil water also plays an important role in the way different tree species respond to drought and may override previous factors. In boreal forest, rooting depth and the ability to use deeper soil water do not play a main role in the way trees respond to drought because the majority of fine root biomass is found near the soil surface and is drastically reduced below 40 cm, as it was observed at our site and nearby forests (Finér et al., 2007; Helmisaari et al., 2007; Persson, 1983; Solly et al., 2018). However, differences among species in total root biomass and root density distribution are likely factors that contribute more to species-specific drought response. In general, pine has an overall higher fine root biomass and higher fine root density in the top 15 cm of the soil profile compared to spruce (Finér et al., 2007). Additionally, root biomass increases with time at a greater rate in pine compared to spruce (Børja et al., 2008; Finér et al., 2007). This would result in higher root-to-leaf area ratio for pine, and facilitate water extraction under a given soil moisture (Ewers et al., 2000). Thus, it appears that pine may be better adapted to take advantage of the small but frequent rain events during the two major drought periods in 2018, supporting our second hypothesis that pine trees are more resilient to drought stress than spruce trees, especially in the more water-limited upland locations.

It is also known that trees of different size respond differently to drought (Bennett et al., 2015; Pretzsch et al., 2018; Stovall et al., 2019). At a global scale, Bennett et al. (2015) reported that larger trees are more sensitive to drought, yet later studies show that sensitivity to drought is independent of tree size (Pretzsch et al., 2018; Stovall et al., 2019). However, most of these previous studies have been conducted in temperate forests below 50°N , where precipitation patterns differ and drought is more clearly defined (Slette et al., 2019). In this study, we observed a nonlinear response of Q to increase in D_z (Appendix S5), and when Q was normalized for variations in VPD, Q_{DZ} was lower during severe drought across all tree sizes (Figure 4), suggesting an ecosystem-level regulation mechanism in northern boreal forests during severe drought. Q_{DZ} did not differ

between the two species (F -Ratio = 0.77, $p = 0.59$). Our analyses (Appendix S4) show (F -Ratio = 6.63, $p < 0.0001$) that small and large pine and spruce trees responded differently to the severe drought periods in 2018. For pine trees, the reduction in Q_{DZ} during severe drought periods in 2018 was more pronounced in large compared to medium and small trees, consistent with our hypothesis that larger trees are more sensitive to drought than smaller trees. In contrast, and opposite to our hypothesis, larger spruce trees appeared less sensitive to drought than smaller trees, indicated by a greater reduction Q_{DZ} in small compared to large spruce trees (Figure 4). This may be partially explained by tree size, water demand, and the relationship between total tree volume and its sapwood area volume, which can act as a buffer for transpiration during short periods of drought (McCulloh et al., 2014; Meinzer et al., 2003). Age- and tree size-related reductions in stomatal conductance and net CO_2 assimilation rates have been documented in pine and spruce (Niinemets, 2002). Overall, lower stomatal conductance and assimilation rates in larger and older pine and spruce seem to increase tolerance to higher water potentials between the soil and the needles under normal environmental conditions (Niinemets, 2002), but it is not well understood if this will hold true under environmental conditions associated with severe drought. At the root level, tree size is also related to root distribution, with larger trees having greater total fine root biomass which in turn may provide better access to soil water when soil moisture in the top soil layers becomes limiting (Canadell et al., 1996; Persson, 1983), yet this needs to be weighed against larger water use due to larger leaf area. Given these species- and size-specific effects on whole-tree transpiration in response to drought, changes in forest stand structure, either through forest management practices or natural disturbances (i.e., wildfire, thinning, clearcutting), could lead to unforeseen large cascading effects on the water balance of headwater catchments in high-latitude boreal forests.

Topographic position is also often considered a strong driving variable in how trees respond to drought (Hawthorne & Miniati, 2018; Roland et al., 2019), with greater mortality frequently observed at higher elevations (i.e., upland locations) as a result of greater water limitation (Seibert et al., 2007), caused by the gravitational gradient moving water toward the lower parts of the watershed (Fetter, 2001; Hillel, 2004). Results from our study partially supported our third hypothesis that trees growing at higher topographical positions will be more affected by drought. Our results showed that there was a difference by topographic position. Both mean Q and Q_{DZ} were higher in higher topographic positions (shoulderslope), compared to lower topographic positions (footslope), and these patterns were observed in all studied years. Nonetheless, after accounting for the differences by topographic position, it was observed that Q_{DZ} reductions were species-specific. At higher topographical locations, pine showed the greatest reduction in Q_{DZ} during the severe drought periods in 2018 (Figure 5), suggesting stronger regulation mechanisms compared to spruce. Conversely, at lower topographical positions, the greatest reduction in Q_{DZ} was observed in spruce trees (Figure 5). A possible explanation for the opposite responses, is that each species showed the greater

response in the location to which it is best suited. These findings are consistent with previous studies that have shown the distribution of pine and spruce commonly follows species-specific adaptations to soil type and nutrient concentration patterns according to their expected age- and size-related stomatal conductance and age-related CO_2 assimilation rates (Martínez & García, 2017; Niinemets, 2002). Pine tends to establish in dryer and more nutrient-poor locations, and spruce is more frequently observed in mesic, nutrient-rich sites (Sutinen & Middleton, 2020). Our results suggest that each species responded most to the drought in the location for which is best adapted. Thus, these findings provide further evidence on how topography may influence the response of boreal trees to drought (Peng et al., 2011), highlighting the need to account for species-specific responses to severe drought along small-scale topographical gradients, and suggesting that three-dimensional scale models may be needed to estimate biosphere-atmosphere fluxes over such ecosystems.

5 | CONCLUSION

This study takes advantage of a large network of tree-level measurements of transpiration to assess how trees growing in a headwater catchment in northern Sweden responded to the historic 2018 summer drought. Despite the drought being one of the most severe in northern Europe and the Fennoscandian peninsula during the past 250 years, whole-tree transpiration remained largely unaffected. Such a finding led us to reject our first hypothesis that tree transpiration was reduced during the historic 2018 drought. However, the lack of response in whole-tree transpiration may, in part, be due to the continuous presence of small precipitation events, and overcast conditions, and stomatal response to VPD, together maintaining a relatively invariant interannual transpiration rates regardless of precipitation amounts. After normalizing whole-tree transpiration for mean daily D_z (Q_{DZ}), thus producing an index of mean crown conductance, we observed a significant reduction in Q_{DZ} for both species in 2018 compared to 2017 and 2019, demonstrating that indeed, stomata regulated transpiration against increasing VPD during the 2018 drought. Moreover, the reduction in Q_{DZ} during severe drought periods of 2018, differed among tree species, tree size, and topographical positions. The reduction in Q_{DZ} during severe drought periods in 2018 was more pronounced in large pine trees compared to medium and small trees, which supports our second hypothesis that larger trees are more sensitive to drought than smaller trees. However, the opposite was observed for spruce trees where larger trees appeared less sensitive to drought compared to smaller trees. Lastly, our results provide qualified support for our third hypothesis that topography plays an important role in how trees respond to drought; the response varied among species, consistent with the sites to which each is best suited. Taken together, our study adds to the limited data available for assessing how whole-tree transpiration in high-latitude ($>50^\circ N$) Fennoscandian boreal forests might respond to future climate

scenarios, and the role of frequently occurring overcast conditions and precipitation on drought response. Furthermore, our results highlight the importance of accounting for variation in the responses to summer drought of different species, tree size, and topographical locations, suggesting increased accuracy if these factors are incorporated, into preferably, watershed models when predicting how these ecosystems will respond to projected increases in summer drought conditions.

ACKNOWLEDGEMENTS

The leading author would like to express sincere gratitude for all the guidance, leadership, and support to our colleague, friend, and mentor Niles Hasselquist, who passed away during the review process. We thank the research staff at the Svartberget Research Station and ICOS Sweden for their help in the establishment and collection of data presented in this paper. This research has been supported by the Swedish Research Council (VR, grant no. 2015-04791), the Knut and Alice Wallenberg Foundation (grant no. 2015.0047), and the Kempe Foundation. Additionally, this project has received funding from the European Union's Horizon 2020 research and innovation programme under the grant agreement No. 871126 (eLTER PPP) and 871128 (eLTER PLUS). The long-term data record has been funded by the Swedish University of Agricultural Sciences and Swedish Research Council (SITES) and other sources including Formas, Future Forests, and SKB. Financial support for Ram Oren was provided by the Erkki Visiting Professor Programme of the Jane and Aatos Erkki 375th Anniversary Fund through the University of Helsinki.

DATA AVAILABILITY STATEMENT

All environmental data is available at the ICOS-Carbon portal: <https://www.icos-cp.eu/data-services/about-data-portal>. Whole-tree transpiration for pine and spruce, data for allometric equations (sapwood area, basal area, sapwood depth), and data describing site characteristics (basal area, species density) is the following data depository link: https://github.com/joseagl/boreal_drought.

ORCID

Jose Gutierrez Lopez  <https://orcid.org/0000-0002-2756-7555>

Ram Oren  <https://orcid.org/0000-0002-5654-1733>

REFERENCES

- Angert, A., Biraud, S., Bonfils, C., Henning, C. C., Buermann, W., Pinzon, J., Pinzon, J., Tucker, C. J., & Fung, I. (2005). Drier summers cancel out the CO₂ uptake enhancement induced by warmer springs. *Proceedings of the National Academy of Sciences of the United States of America*, *102*, 10823–10827.
- Baldocchi, D., Kelliher, F. M., Black, T. A., & Jarvis, P. (2000). Climate and vegetation controls on boreal zone energy exchange. *Global Change Biology*, *6*(S1), 69–83. <https://doi.org/10.1046/j.1365-2486.2000.06014.x>
- Barber, V. A., Juday, G. P., & Finney, B. P. (2000). Reduced growth of Alaskan white spruce in the twentieth century from temperature-induced drought stress. *Nature*, *405*(6787), 668–673. <https://doi.org/10.1038/35015049>
- Bennett, A. C., McDowell, N. G., Allen, C. D., & Anderson-Teixeira, K. J. (2015). Larger trees suffer most during drought in forests worldwide. *Nature Plants*, *1*(10), 15139. <https://doi.org/10.1038/nplants.2015.139>
- Berdanier, A. B., Miniati, C. F., & Clark, J. S. (2016). Predictive models for radial sap flux variation in coniferous, diffuse-porous and ring-porous temperate trees. *Tree Physiology*, *36*(8), 932–941. <https://doi.org/10.1093/treephys/tpw027>
- Bonan, G. B. (2008). Forests and climate change: Forcings, feedbacks, and the climate benefits of forests. *Science*, *320*, 1444–1449.
- Boonstra, R., Andreassen, H. P., Boutin, S., Hušek, J., Ims, R. A., Krebs, C. J., Skarpe, C., & Wabakken, P. (2016). Why do the boreal forest ecosystems of northwestern Europe differ from those of western North America? *BioScience*, *66*(9), 722–734. <https://doi.org/10.1093/biosci/biw080>
- Børja, I., De Wit, H. A., Steffenrem, A., & Majdi, H. (2008). Stand age and fine root biomass, distribution and morphology in a Norway spruce chronosequence in southeast Norway. *Tree Physiology*, *28*(5), 773–784. <https://doi.org/10.1093/treephys/28.5.773>
- Bradshaw, C. J. A., & Warkentin, I. G. (2015). Global estimates of boreal forest carbon stocks and flux. *Global and Planetary Change*, *128*, 24–30. <https://doi.org/10.1016/j.gloplacha.2015.02.004>
- Bradshaw, C. J. A., Warkentin, I. G., & Sodhi, N. S. (2009). Urgent preservation of boreal carbon stocks and biodiversity. *Trends in Ecology & Evolution*, *24*(10), 541–548. <https://doi.org/10.1016/j.tree.2009.03.019>
- Canadell, J., Jackson, R. B., Ehleringer, J. B., Mooney, H. A., Sala, O. E., & Schulze, E. D. (1996). Maximum rooting depth of vegetation types at the global scale. *Oecologia*, *108*(4), 583–595. <https://doi.org/10.1007/BF00329030>
- Caylor, K. K., & Dragoni, D. (2009). Decoupling structural and environmental determinants of sap velocity: Part I. Methodological development. *Agricultural and Forest Meteorology*, *149*(3), 559–569. <https://doi.org/10.1016/j.agrformet.2008.10.006>
- Čermák, J., Cienciala, E., Kučera, J., Lindroth, A., & Bednářová, E. (1995). Individual variation of sap-flow rate in large pine and spruce trees and stand transpiration: A pilot study at the central NOPEX site. *Journal of Hydrology*, *168*(1), 17–27. [https://doi.org/10.1016/0022-1694\(94\)02657-W](https://doi.org/10.1016/0022-1694(94)02657-W)
- Chalita, S., & Le Treut, H. (1994). The albedo of temperate and boreal forest and the Northern Hemisphere climate: A sensitivity experiment using the LMD GCM. *Climate Dynamics*, *10*(4–5), 231–240.
- Chen, D., Loboda, T. V., He, T., Zhang, Y., & Liang, S. (2018). Strong cooling induced by stand-replacing fires through albedo in Siberian larch forests. *Scientific Reports*, *8*(1), 4821. <https://doi.org/10.1038/s41598-018-23253-1>
- Choi, W., & Kim, K.-Y. (2018). Physical mechanism of spring and early summer drought over North America associated with the boreal warming. *Scientific Reports*, *8*(1), 7533. <https://doi.org/10.1038/s41598-018-25932-5>
- Christidis, N., Jones, G. S., & Stott, P. A. (2015). Dramatically increasing chance of extremely hot summers since the 2003 European heatwave. *Nature Climate Change*, *5*(1), 46–50. <https://doi.org/10.1038/nclimate2468>
- Cienciala, E., Kučera, J., & Lindroth, A. (1999). Long-term measurements of stand water uptake in Swedish boreal forest. *Agricultural and Forest Meteorology*, *123*, 547–554. [https://doi.org/10.1016/S0168-1923\(99\)00122-7](https://doi.org/10.1016/S0168-1923(99)00122-7)
- Cienciala, E., Kučera, J., Lindroth, A., Čermák, J., Grelle, A., & Halldin, S. (1997). Canopy transpiration from a boreal forest in Sweden during a dry year. *Agricultural and Forest Meteorology*, *86*(3), 157–167. [https://doi.org/10.1016/S0168-1923\(97\)00026-9](https://doi.org/10.1016/S0168-1923(97)00026-9)
- Cleveland, W. S. (1979). Robust locally weighted regression and smoothing scatterplots. *Journal of the American Statistical Association*, *74*(368), 829–836.
- Cleveland, W. S. (1981). Lowess – A program for smoothing scatterplots by robust locally weighted regression. *American Statistician*, *35*(1), 54. <https://doi.org/10.2307/2683591>

- Dai, A. (2013). Increasing drought under global warming in observations and models. *Nature Climate Change*, 3(1), 52–58. <https://doi.org/10.1038/nclimate1633>
- Damou, G., Simonneau, T., Cochard, H., & Urban, L. (2010). An overview of models of stomatal conductance at the leaf level. *Plant, Cell & Environment*, 33(9), 1419–1438. <https://doi.org/10.1111/j.1365-3040.2010.02181.x>
- Dang, Q.-L., Margolis, H. A., Coyea, M. R., Sy, M., & Collatz, G. J. (1997). Regulation of branch-level gas exchange of boreal trees: roles of shoot water potential and vapor pressure difference. *Tree Physiology*, 17(8–9), 521–535. <https://doi.org/10.1093/treephys/17.8-9.521>
- D'Orangeville, L., Maxwell, J., Kneeshaw, D., Pederson, N., Duchesne, L., Logan, T., Houle, D., Arseneault, D., Beier, C. M., Bishop, D. A., Druckenbrod, D., Fraver, S., Girard, F., Halman, J., Hansen, C., Hart, J. L., Hartmann, H., Kaye, M., Leblanc, D., ... Phillips, R. P. (2018). Drought timing and local climate determine the sensitivity of eastern temperate forests to drought. *Global Change Biology*, 24(6), 2339–2351. <https://doi.org/10.1111/gcb.14096>
- Ewers, B. E., & Oren, R. (2000). Analyses of assumptions and errors in the calculation of stomatal conductance from sap flux measurements. *Tree Physiology*, 20(9), 579–589. <https://doi.org/10.1093/treephys/20.9.579>
- Ewers, B. E., Oren, R., Albaugh, T. J., & Dougherty, P. M. (1999). Carry-over effects of water and nutrient supply on water use of *Pinus taeda*. *Ecological Applications*, 9(2), 513–525. [10.1890/1051-0761\(1999\)009\[0513:COEOWA\]2.0.CO;2](https://doi.org/10.1890/1051-0761(1999)009[0513:COEOWA]2.0.CO;2)
- Ewers, B. E., Oren, R., & Sperry, J. S. (2000). Influence of nutrient versus water supply on hydraulic architecture and water balance in *Pinus taeda*. *Plant, Cell & Environment*, 23(10), 1055–1066. <https://doi.org/10.1046/j.1365-3040.2000.00625.x>
- Fetter, C. W. (2001). *Applied hydrogeology* (4th ed.). Prentice Hall.
- Finér, L., Helmisaari, H. S., Löhmus, K., Majdi, H., Brunner, I., Børja, I., & Vanguelova, E. (2007). Variation in fine root biomass of three European tree species: Beech (*Fagus sylvatica* L.), Norway spruce (*Picea abies* L. Karst.), and Scots pine (*Pinus sylvestris* L.). *Plant Biosystems*, 141(3), 394–405. <https://doi.org/10.1080/11263500701625897>
- Flo, V., Martínez-Vilalta, J., Steppe, K., Schuldt, B., & Poyatos, R. (2019). A synthesis of bias and uncertainty in sap flow methods. *Agricultural and Forest Meteorology*, 271, 362–374. <https://doi.org/10.1016/j.agrformet.2019.03.012>
- Gartner, K., Nadezhdina, N., Englisch, M., Čermak, J., & Leitgeb, E. (2009). Sap flow of birch and Norway spruce during the European heat and drought in summer 2003. *Forest Ecology and Management*, 258(5), 590–599. <https://doi.org/10.1016/j.foreco.2009.04.028>
- Gómez-Gener, L., Lupon, A., Laudon, H., & Sponseller, R. A. (2020). Drought alters the biogeochemistry of boreal stream networks. *Nature Communications*, 11(1), 1795. <https://doi.org/10.1038/s41467-020-15496-2>
- Goodale, C. L., Apps, M. J., Birdsey, R. A., Field, C. B., Heath, L. S., Houghton, R. A., Jenkins, J. C., Kohlmaier, G. H., Kurz, W., Liu, S., Nabuurs, G.-J., Nilsson, S., & Shvidenko, A. Z. (2002). Forest carbon sinks in the northern hemisphere. *Ecological Applications*, 12(3), 891–899. [10.1890/1051-0761\(2002\)012\[0891:Fcsitn\]2.0.CO;2](https://doi.org/10.1890/1051-0761(2002)012[0891:Fcsitn]2.0.CO;2)
- Goude, M., Nilsson, U., & Holmström, E. (2019). Comparing direct and indirect leaf area measurements for Scots pine and Norway spruce plantations in Sweden. *European Journal of Forest Research*, 138(6), 1033–1047. <https://doi.org/10.1007/s10342-019-01221-2>
- Granier, A. (1985). Une nouvelle méthode pour la mesure du flux de sève brute dans le tronc des arbres. *Annals of Forest Science*, 42(2), 193–200. <https://doi.org/10.1051/forest:19850204>
- Granier, A. (1987). Evaluation of transpiration in a Douglas-Fir stand by means of sap flow measurements. *Tree Physiology*, 3(4), 309–319.
- Granier, A., Anfodillo, T., Sabatti, M., Cochard, H., Dreyer, E., Tomasi, M., Valentini, R., & Breda, N. (1994). Axial and radial water-flow in trunks of oak trees – A quantitative and qualitative-analysis. *Tree Physiology*, 14(12), 1383–1396.
- Gutiérrez López, J. A. (2015). Construction of heat dissipation probes to estimate sap flow. <https://doi.org/10.13140/RG.2.1.1181.2004>
- Hari, V., Rakovec, O., Markonis, Y., Hanel, M., & Kumar, R. (2020). Increased future occurrences of the exceptional 2018–2019 Central European drought under global warming. *Scientific Reports*, 10(1), 12207. <https://doi.org/10.1038/s41598-020-68872-9>
- Hasper, T. B., Wallin, G., Lamba, S., Hall, M., Jaramillo, F., Laudon, H., Linder, S., Medhurst, J. L., Rantfors, M., Sigurdsson, B. D., & Uddling, J. (2016). Water use by Swedish boreal forests in a changing climate. *Functional Ecology*, 30(5), 690–699. <https://doi.org/10.1111/1365-2435.12546>
- Hawthorne, S., & Miniati, C. F. (2018). Topography may mitigate drought effects on vegetation along a hillslope gradient. *Ecohydrology*, 11(1), e1825. <https://doi.org/10.1002/eco.1825>
- Helmisaari, H.-S., Derome, J., Nöjd, P., & Kukkola, M. (2007). Fine root biomass in relation to site and stand characteristics in Norway spruce and Scots pine stands. *Tree Physiology*, 27(10), 1493–1504. <https://doi.org/10.1093/treephys/27.10.1493>
- Hillel, D. (2004). *Introduction to environmental soil physics*. Elsevier Academic Press.
- Hogg, E. H., Brandt, J. P., & Kochtubajda, B. (2002). Growth and dieback of aspen forests in northwestern Alberta, Canada, in relation to climate and insects. *Canadian Journal of Forest Research*, 32(5), 823–832. <https://doi.org/10.1139/x01-152>
- Hogg, E. H., Brandt, J. P., & Michaelian, M. (2008). Impacts of a regional drought on the productivity, dieback, and biomass of western Canadian aspen forests. *Canadian Journal of Forest Research*, 38(6), 1373–1384. <https://doi.org/10.1139/X08-001>
- Huang, K., & Xia, J. (2019). High ecosystem stability of evergreen broadleaf forests under severe droughts. *Global Change Biology*, 25(10), 3494–3503. <https://doi.org/10.1111/gcb.14748>
- ICOS. (2019). Integrated carbon observation system – Svartberget. https://www.icos-sweden.se/station_svartberget.html
- IPCC. (2013). Climate Change 2013: The physical science basis. In T. F. Stocker, D. Qin, G.-K. Plattner, M. Tignor, S. K. Allen, J. Boschung, A. Nauels, Y. Xia, V. Bex, & P. M. Midgley (Eds.), *Contribution of working group I to the fifth assessment report of the Intergovernmental Panel on Climate Change*. Cambridge University Press. 1535 pp.
- Ivarsson, H., & Johnsson, T. (1988). *Stratigraphy of the quaternary deposits in the Nyänges drainage area, within the svartberget forest experimental area and a general geomorphological description of the Vindeln region*. Sveriges Lantbruksuniversitet. ISSN: 0280-4328.
- Kitin, P., Voelker, S. L., Meinzer, F. C., Beekman, H., Strauss, S. H., & Lachenbruch, B. (2010). Tyloses and phenolic deposits in xylem vessels impede water transport in low-lignin transgenic poplars: a study by cryo-fluorescence microscopy. *Plant Physiology*, 154(2), 887–898. <https://doi.org/10.1104/pp.110.156224>
- Kjellström, E. (2004). Recent and future signatures of climate change in Europe. *Ambio*, 33(4/5), 193–198.
- Kozii, N., Haahti, K., Torngern, P., Chi, J., Hasselquist, E. M., Laudon, H., Launiainen, S., Oren, R., Peichl, M., Wallerman, J., & Hasselquist, N. J. (2020). Partitioning growing season water balance within a forested boreal catchment using sap flux, eddy covariance, and a process-based model. *Hydrology and Earth System Sciences*, 24(6), 2999–3014. <https://doi.org/10.5194/hess-24-2999-2020>
- Kropp, H., Lorant, M., Alexander, H. D., Berner, L. T., Natali, S. M., & Spawn, S. A. (2017). Environmental constraints on transpiration and stomatal conductance in a Siberian Arctic boreal forest. *Journal of Geophysical Research: Biogeosciences*, 122(3), 487–497. <https://doi.org/10.1002/2016jg003709>
- Lagergren, F., & Lindroth, A. (2002). Transpiration response to soil moisture in pine and spruce trees in Sweden. *Agricultural and Forest Meteorology*, 112(2), 67–85. [https://doi.org/10.1016/S0168-1923\(02\)00060-6](https://doi.org/10.1016/S0168-1923(02)00060-6)

- Lagergren, F., & Lindroth, A. (2004). Variation in sapflow and stem growth in relation to tree size, competition and thinning in a mixed forest of pine and spruce in Sweden. *Forest Ecology and Management*, 188(1), 51–63. <https://doi.org/10.1016/j.foreco.2003.07.018>
- Lai, C.-T., Katul, G., Oren, R., Ellsworth, D., & Schäfer, K. (2000). Modeling CO₂ and water vapor turbulent flux distributions within a forest canopy. *Journal of Geophysical Research: Atmospheres*, 105(D21), 26333–26351. <https://doi.org/10.1029/2000JD900468>
- Larsen, J. A. (1980). *The boreal ecosystem*. Academic Press.
- Laudon, H., Taberman, I., Ågren, A., Futter, M., Ottosson-Löfvenius, M., & Bishop, K. (2013). The Krycklan Catchment Study—A flagship infrastructure for hydrology, biogeochemistry, and climate research in the boreal landscape. *Water Resources Research*, 49(10), 7154–7158. <https://doi.org/10.1002/wrcr.20520>
- Launiainen, S., Guan, M., Salmivaara, A., & Kieloaho, A. J. (2019). Modeling boreal forest evapotranspiration and water balance at stand and catchment scales: A spatial approach. *Hydrology and Earth System Sciences*, 23(8), 3457–3480. <https://doi.org/10.5194/hess-23-3457-2019>
- Lindroth, A., Holst, J., Linderson, M.-L., Aurela, M., Biermann, T., Heliasz, M., Chi, J., Ibrom, A., Kolari, P., Klemedtsson, L., Krasnova, A., Laurila, T., Lehner, I., Lohila, A., Mammarella, I., Mölder, M., Löfvenius, M. O., Peichl, M., Pilegaard, K., ... Nilsson, M. (2020). Effects of drought and meteorological forcing on carbon and water fluxes in Nordic forests during the dry summer of 2018. *Philosophical Transactions of the Royal Society B: Biological Sciences*, 375(1810), 20190516. <https://doi.org/10.1098/rstb.2019.0516>
- Long, J. N., & Dean, T. J. (1986). Sapwood area of *Pinus contorta* stands as a function of mean size and density. *Oecologia*, 68(3), 410–412.
- Ma, Z., Peng, C., Zhu, Q., Chen, H., Yu, G., Li, W., Zhou, X., Wang, W., & Zhang, W. (2012). Regional drought-induced reduction in the biomass carbon sink of Canada's boreal forests. *Proceedings of the National Academy of Sciences of the United States of America*, 109, 2423–2427.
- Martínez, J., & García, N. (2017). Water potential regulation, stomatal behaviour and hydraulic transport under drought: Deconstructing the iso/anisohydric concept. *Plant, Cell & Environment*, 40(6), 962–976. <https://doi.org/10.1111/pce.12846>
- McCulloh, K. A., Johnson, D. M., Meinzer, F. C., & Woodruff, D. R. (2014). The dynamic pipeline: hydraulic capacitance and xylem hydraulic safety in four tall conifer species. *Plant, Cell & Environment*, 37(5), 1171–1183. <https://doi.org/10.1111/pce.12225>
- McDowell, N., Pockman, W. T., Allen, C. D., Breshears, D. D., Cobb, N., Kolb, T., Plaut, J., Sperry, J., West, A., Williams, D. G., & Yezzer, E. A. (2008). Mechanisms of plant survival and mortality during drought: Why do some plants survive while others succumb to drought? *New Phytologist*, 178(4), 719–739. <https://doi.org/10.1111/j.1469-8137.2008.02436.x>
- McElrone, A. J., Grant, J. A., & Kluepfel, D. A. (2010). The role of tyloses in crown hydraulic failure of mature walnut trees afflicted by apoplexy disorder. *Tree Physiology*, 30(6), 761–772. <https://doi.org/10.1093/Treephys/Tpq026>
- Meinzer, F. C., James, C. D., Goldstein, G., & Woodruff, D. (2003). Whole-tree water transport scales with sapwood capacitance in tropical forest canopy trees. *Plant, Cell & Environment*, 26(7), 1147–1155. <https://doi.org/10.1046/j.1365-3040.2003.01039.x>
- Montwé, D., Isaac-Renton, M., Hamann, A., & Spiecker, H. (2016). Drought tolerance and growth in populations of a wide-ranging tree species indicate climate change risks for the boreal north. *Global Change Biology*, 22(2), 806–815. <https://doi.org/10.1111/gcb.13123>
- MSB. (2017). *Droughts and wildfires in Sweden: past variation and future projection (MSB1112-June2017)*. <https://rib.msb.se/filer/pdf/28280.pdf>
- Niinemet, Ü. (2002). Stomatal conductance alone does not explain the decline in foliar photosynthetic rates with increasing tree age and size in *Picea abies* and *Pinus sylvestris*. *Tree Physiology*, 22(8), 515–535. <https://doi.org/10.1093/treephys/22.8.515>
- Oishi, A. C., Oren, R., Novick, K. A., Palmroth, S., & Katul, G. G. (2010). Interannual invariability of forest evapotranspiration and its consequence to water flow downstream. *Ecosystems*, 13(3), 421–436. <https://doi.org/10.1007/s10021-010-9328-3>
- Oltchev, A., Cermak, J., Nadezhdina, N., Tatarinov, F., Tishenko, A., Ibrom, A., & Gravenhorst, G. (2002). Transpiration of a mixed forest stand: Field measurements and simulation using SVAT models. *Boreal Environment Research*, 7, 389–397.
- Pan, Y., Birdsey, R. A., Fang, J., Houghton, R., Kauppi, P. E., Kurz, W. A., Phillips, O. L., Shvidenko, A., Lewis, S. L., Canadell, J. G., Ciais, P., Jackson, R. B., Pacala, S. W., McGuire, A. D., Piao, S., Rautiainen, A., Sitch, S., & Hayes, D. (2011). A large and persistent carbon sink in the world's forests. *Science*, 333, 988–993.
- Park Williams, A., Allen, C. D., Macalady, A. K., Griffin, D., Woodhouse, C. A., Meko, D. M., Swetnam, T. W., Rauscher, S. A., Seager, R., Grissino-Mayer, H. D., Dean, J. S., Cook, E. R., Gangogadamage, C., Cai, M., & McDowell, N. G. (2013). Temperature as a potent driver of regional forest drought stress and tree mortality. *Nature Climate Change*, 3(3), 292–297. <https://doi.org/10.1038/nclimate1693>
- Peng, C., Ma, Z., Lei, X., Zhu, Q., Chen, H., Wang, W., Liu, S., Li, W., Fang, X., & Zhou, X. (2011). A drought-induced pervasive increase in tree mortality across Canada's boreal forests. *Nature Climate Change*, 1, 467. <https://doi.org/10.1038/nclimate1293>
- Persson, H. Å. (1983). The distribution and productivity of fine roots in boreal forests. *Plant and Soil*, 71(1), 87–101. <https://doi.org/10.1007/BF02182644>
- Peters, R. L., Fonti, P., Frank, D. C., Poyatos, R., Pappas, C., Kahmen, A., Carraro, V., Prendin, A. L., Schneider, L., Baltzer, J. L., Baron-Gafford, G. A., Dietrich, L., Heinrich, I., Minor, R. L., Sonntag, O., Matheny, A. M., Wightman, M. G., & Steppe, K. (2018). Quantification of uncertainties in conifer sap flow measured with the thermal dissipation method. *New Phytologist*, 219(4), 1283–1299. <https://doi.org/10.1111/nph.15241>
- Phillips, N., & Oren, R. (1998). A comparison of daily representations of canopy conductance based on two conditional time-averaging methods and the dependence of daily conductance on environmental factors. *Annals of Forest Science*, 55(1–2), 217–235.
- Pretzsch, H., Schütze, G., & Biber, P. (2018). Drought can favour the growth of small in relation to tall trees in mature stands of Norway spruce and European beech. *Forest Ecosystems*, 5(1), 20. <https://doi.org/10.1186/s40663-018-0139-x>
- Price, D. T., Alfaro, R. I., Brown, K. J., Flannigan, M. D., Fleming, R. A., Hogg, E. H., Girardin, M. P., Lakusta, T., Johnston, M., McKenney, D. W., Pedlar, J. H., Stratton, T., Sturrock, R. N., Thompson, I. D., Trofymow, J. A., & Venier, L. A. (2013). Anticipating the consequences of climate change for Canada's boreal forest ecosystems. *Environmental Reviews*, 21(4), 322–365. <https://doi.org/10.1139/er-2013-0042>
- Roland, C. A., Schmidt, J. H., Winder, S. G., Stehn, S. E., & Nicklen, E. F. (2019). Regional variation in interior Alaskan boreal forests is driven by fire disturbance, topography, and climate. *Ecological Monographs*, 89(3), e01369. <https://doi.org/10.1002/ecm.1369>
- Rowland, L., da Costa, A. C. L., Galbraith, D. R., Oliveira, R. S., Binks, O. J., Oliveira, A. A. R., Pullen, A. M., Doughty, C. E., Metcalfe, D. B., Vasconcelos, S. S., Ferreira, L. V., Malhi, Y., Grace, J., Mencuccini, M., & Meir, P. (2015). Death from drought in tropical forests is triggered by hydraulics not carbon starvation. *Nature*, 528(7580), 119–+. <https://doi.org/10.1038/nature15539>
- Schäfer, K. V. R., Oren, R., & Tenhunen, J. D. (2000). The effect of tree height on crown level stomatal conductance. *Plant, Cell & Environment*, 23(4), 365–375. <https://doi.org/10.1046/j.1365-3040.2000.00553.x>
- Schuldt, B., Buras, A., Arend, M., Vitasse, Y., Beierkuhnlein, C., Damm, A., Gharun, M., Grams, T. E. E., Hauck, M., Hajek, P., Hartmann, H., Hiltbrunner, E., Hoch, G., Holloway-Phillips, M., Körner, C., Larysch,

- E., Lübbe, T., Nelson, D. B., Rammig, A., ... Kahmen, A. (2020). A first assessment of the impact of the extreme 2018 summer drought on Central European forests. *Basic and Applied Ecology*, 45, 86–103. <https://doi.org/10.1016/j.baae.2020.04.003>
- Seibert, J., Stendahl, J., & Sørensen, R. (2007). Topographical influences on soil properties in boreal forests. *Geoderma*, 141(1–2), 139–148. <https://doi.org/10.1016/j.geoderma.2007.05.013>
- Silva, L. C. R., Anand, M., & Leithead, M. D. (2010). Recent widespread tree growth decline despite increasing atmospheric CO₂. *PLoS One*, 5(7), e11543. <https://doi.org/10.1371/journal.pone.0011543>
- Slette, I. J., Post, A. K., Awad, M., Even, T., Punzalan, A., Williams, S., Smith, M. D., & Knapp, A. K. (2019). How ecologists define drought, and why we should do better. *Global Change Biology*, 25(10), 3193–3200. <https://doi.org/10.1111/gcb.14747>
- Soja, A. J., Tchepakova, N. M., French, N. H. F., Flannigan, M. D., Shugart, H. H., Stocks, B. J., Sukhinin, A. I., Parfenova, E. I., Chapin, F. S., & Stackhouse, P. W. (2007). Climate-induced boreal forest change: Predictions versus current observations. *Global and Planetary Change*, 56(3), 274–296. <https://doi.org/10.1016/j.gloplacha.2006.07.028>
- Solly, E. F., Brunner, I., Helmisaari, H.-S., Herzog, C., Leppälammikujansuu, J., Schöning, I., Schruppf, M., Schweingruber, F. H., Trumbore, S. E., & Hagedorn, F. (2018). Unravelling the age of fine roots of temperate and boreal forests. *Nature Communications*, 9(1), 3006. <https://doi.org/10.1038/s41467-018-05460-6>
- Stovall, A. E. L., Shugart, H., & Yang, X. (2019). Tree height explains mortality risk during an intense drought. *Nature Communications*, 10(1), 4385. <https://doi.org/10.1038/s41467-019-12380-6>
- Sutinen, R., & Middleton, M. (2020). Soil water drives distribution of northern boreal conifers *Picea abies* and *Pinus sylvestris*. *Journal of Hydrology*, 588, 125048. <https://doi.org/10.1016/j.jhydrol.2020.125048>
- Tor-ngern, P., Oren, R., Oishi, A. C., Uebelherr, J. M., Palmroth, S., Tarvainen, L., Ottosson-Löfvenius, M., Linder, S., Domec, J.-C., & Näsholm, T. (2017). Ecophysiological variation of transpiration of pine forests: Synthesis of new and published results. *Ecological Applications*, 27(1), 118–133. <https://doi.org/10.1002/eap.1423>
- van Genuchten, M. T. (1980). A closed-form equation for predicting the hydraulic conductivity of unsaturated soils. *Soil Science Society of America Journal*, 44(5), 892–898. <https://doi.org/10.2136/sssaj1980.03615995004400050002x>
- Van Loon, A. F., Gleeson, T., Clark, J., Van Dijk, A. I. J. M., Stahl, K., Hannaford, J., Di Baldassarre, G., Teuling, A. J., Tallaksen, L. M., Uijlenhoet, R., Hannah, D. M., Sheffield, J., Svoboda, M., Verbeiren, B., Wagener, T., Rangelcroft, S., Wanders, N., & Van Lanen, H. A. J. (2016). Drought in the Anthropocene. *Nature Geoscience*, 9(2), 89–91. <https://doi.org/10.1038/ngeo2646>
- Vicente-Serrano, S. M., Beguería, S., & López-Moreno, J. I. (2010). A multiscalar drought index sensitive to global warming: The standardized precipitation evapotranspiration index. *Journal of Climate*, 23(7), 1696–1718. <https://doi.org/10.1175/2009jcli2909.1>
- Vörösmarty, C. J., McIntyre, P. B., Gessner, M. O., Dudgeon, D., Prusevich, A., Green, P., Glidden, S., Bunn, S. E., Sullivan, C. A., Liermann, C. R., & Davies, P. M. (2010). Global threats to human water security and river biodiversity. *Nature*, 467(7315), 555–561. <https://doi.org/10.1038/nature09440>
- Walker, X. J., Mack, M. C., & Johnstone, J. F. (2015). Stable carbon isotope analysis reveals widespread drought stress in boreal black spruce forests. *Global Change Biology*, 21(8), 3102–3113. <https://doi.org/10.1111/gcb.12893>
- Ward, E. J., Oren, R., Seok Kim, H., Kim, D., Tor-ngern, P., Ewers, B. E., & Schäfer, K. V. R. (2018). Evapotranspiration and water yield of a pine-broadleaf forest are not altered by long-term atmospheric [CO₂] enrichment under native or enhanced soil fertility. *Global Change Biology*, 24(10), 4841–4856. <https://doi.org/10.1111/gcb.14363>
- Way, D. A., Crawley, C., & Sage, R. F. (2013). A hot and dry future: Warming effects on boreal tree drought tolerance. *Tree Physiology*, 33(10), 1003–1005. <https://doi.org/10.1093/treephys/tpt092>
- Wengert, E. M. (1976). A quick method to distinguish aspen heartwood and sapwood. *Wood and Fiber*, 8(2).
- Wullschlegel, S. D., & King, A. W. (2000). Radial variation in sap velocity as a function of stem diameter and sapwood thickness in yellow-poplar trees. *Tree Physiology*, 20(8), 511–518.
- Zotarelli, L., Dukes, M. D., Romero, C., Migliaccio, K., & Morgan, K. (2015). Step by step calculation of the Penman-Monteith evapotranspiration (FAO-56-Method) 1.

SUPPORTING INFORMATION

Additional supporting information may be found online in the Supporting Information section.

How to cite this article: Gutierrez Lopez J, Tor-ngern P, Oren R, Kozii N, Laudon H, Hasselquist NJ. How tree species, tree size, and topographical location influenced tree transpiration in northern boreal forests during the historic 2018 drought. *Global Change Biol.* 2021;27:3066–3078. <https://doi.org/10.1111/gcb.15601>